

## Supporting Information

### ***Eldfellite* NaV(SO<sub>4</sub>)<sub>2</sub> as a versatile cathode insertion host for Li-ion and Na-ion batteries**

Shashwat Singh,<sup>a</sup> Deobrat Singh,<sup>b</sup> Rajeev Ahuja,<sup>b,c,d</sup> Maximilian Fichtner,<sup>e,f</sup> Prabeer Barpanda<sup>\*a,c</sup>

a. Faraday Materials Laboratory (FaMaL), Materials Research Centre, Indian Institute of Science, Bangalore 560012, India

b. Condensed Matter Theory Group, Materials Theory Division, Department of Physics and Astronomy, Uppsala University, Box 516, 75120 Uppsala, Sweden

c. Applied Materials Physics, Department of Materials Science and Engineering, Royal Institute of Technology (KTH), Stockholm S-100 44, Sweden

d. Department of Physics, Indian Institute of Technology Ropar, Rupnagar, Punjab 140001, India

e. Helmholtz Institute Ulm (HIU), Electrochemical Energy Storage, Ulm 89081, Germany

f. Institute of Nanotechnology, Karlsruhe Institute of technology (KIT), Karlsruhe 76021, Germany

\*Corresponding author.

E-mail address: [prabeer@iisc.ac.in](mailto:prabeer@iisc.ac.in)

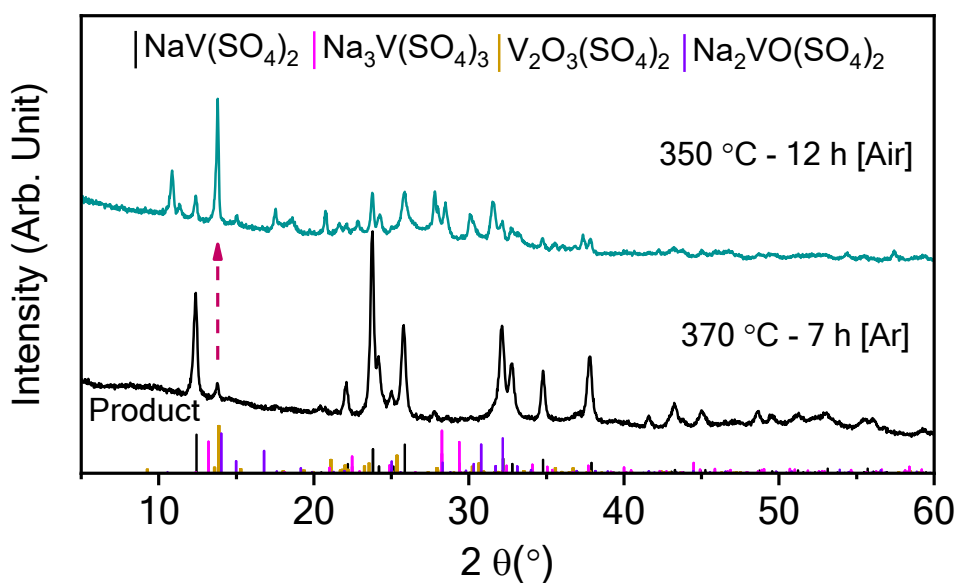


**Fig. S1.** Powder XRD pattern comparison after heat treatment of intermediate powder in Ar (in tube furnace) and air (in muffle furnace) atmosphere. Dashed arrow indicates the growth of the impurity peak. In both cases, 10 % excess oxalic acid was added during synthesis. The reference Bragg positions of candidate impurity phases have been indicated.

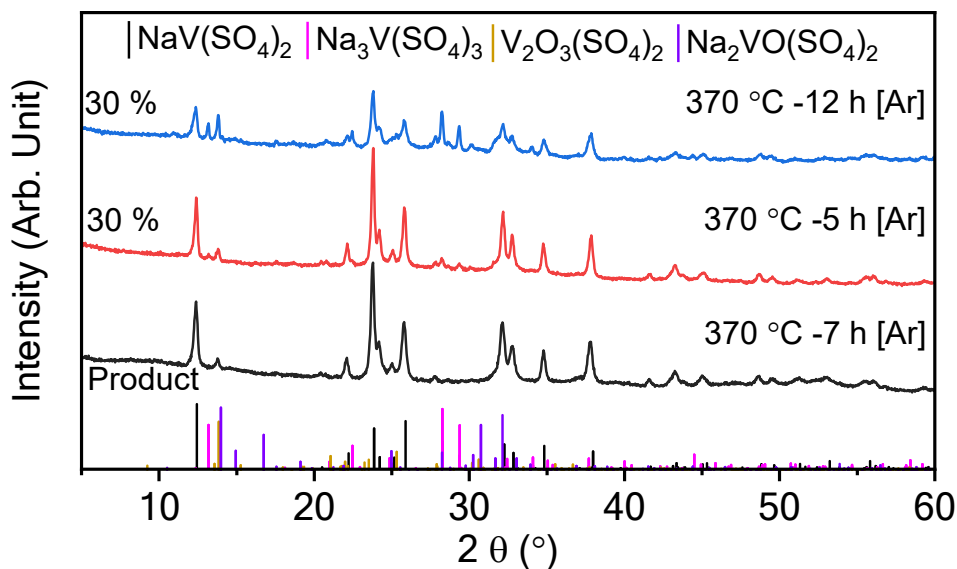


**Fig. S2.** Powder XRD pattern comparison after heat treatment of intermediate powders in Ar (in tube furnace). Percentage indicates the excess Oxalic acid added into the solution. In the pristine product, 10 % excess oxalic acid was added. Magenta colored tics correspond to the reference pattern of  $\text{Na}_3\text{V}(\text{SO}_4)_2$  phase which has notably increased with excess addition of Oxalic acid. The reference Bragg positions of other possible impurity phases have been indicated.

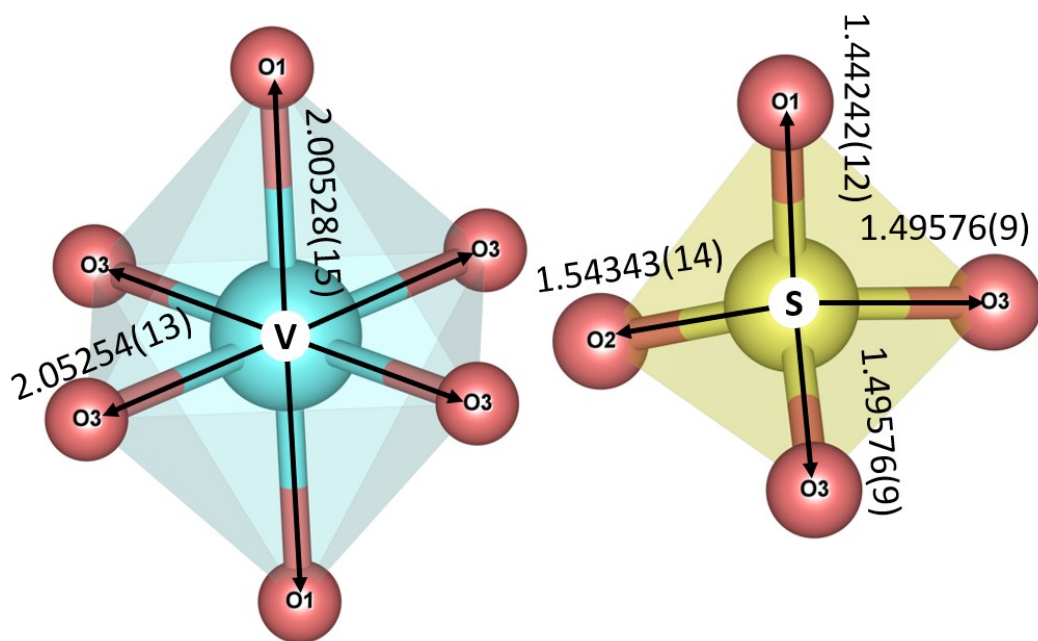


**Fig. S3.** Bond distances, in Å, between vertices and central atom of  $\text{VO}_6$  and  $\text{SO}_4$  polyhedra estimated from Rietveld analysis of *monoclinic*  $\text{NaV}(\text{SO}_4)_2$ . The central atom is indicated in white solid circle.  $\text{VO}_6$  has only two distinct type of oxygen- O1 and O3.  $\text{SO}_4$  has three types of oxygen- O1, O2 and O3. O2 (oxygen) is not shared among these two polyhedral units.

**Table S1.** Bond length, Baur's distortion index and bond angle variance<sup>1</sup> of  $\text{VO}_6$  and  $\text{SO}_4$

polyhedra of *monoclinic* NaV(SO<sub>4</sub>)<sub>2</sub> obtained from CIF generated after Rietveld analysis. There are only one type of Na, V, and S atom, while 3 different types of oxygen atoms- O1, O2 and O3 are present per unit formula. Vesta software was used for structural illustration.

SO <sub>4</sub>	Bond length (Å)	Volume (Å <sup>3</sup> )	Distortion Index	Quadratic Elongation	Bond angle variance (° <sup>2</sup> )	Effective Coordination Number
S1-O1	1.44242(12)	1.7009	0.01737	1.0051	15.2008	3.9065
S1-O2	1.54343(14)					
S1-O3	1.49576(9)					
S1-O3	1.49576(9)					

VO <sub>6</sub>	Bond length (Å)	Volume (Å <sup>3</sup> )	Distortion Index	Quadratic Elongation	Bond angle variance (° <sup>2</sup> )	Effective Coordination Number
2 × V1-O1	2.00528(15)	11.1990	0.01031	1.0041	14.3891	5.9735
4 × V1-O3	2.05254(13)					

**Table S2.** Position and energy of minimum energy sites (Na1 and i1) and saddle points (s1 and s2) in NaV(SO<sub>4</sub>)<sub>2</sub> framework, estimated using softBV package.

Site	Multiplicity	x	y	z	Energy (eV)
Na1	2	0	0	0.5	0
i1	4	0.226	0.5	0.264	0.172
s1	4	0.143	0	0.625	0.711
s2	8	0.143	0.283	0.389	1.247

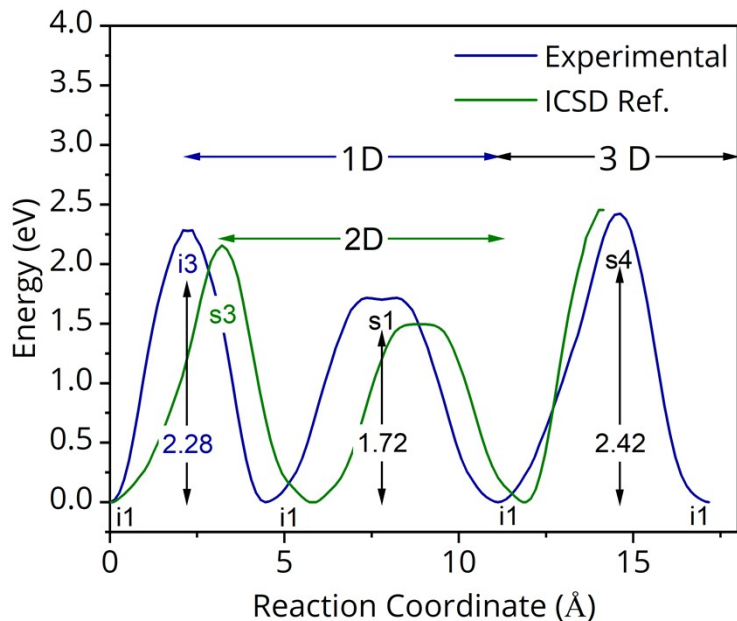


**Fig. S4.**  $\text{Li}^+$  ion migration pathway in  $\text{NaV}(\text{SO}_4)_2$ . The comparative activation energy values are, from left to right, for guest  $\text{Li}^+$ . Interstitial position is denoted as i1 and saddle points are denoted as S1, S3, and S4. The reference structural model offers a 2D and 3D ionic migration pathway at migration barrier of 2.155 eV and 2.454 eV, respectively. However, the 3D migration pathway for  $\text{Li}^+$  migration is interesting because such path is restricted for  $\text{Na}^+$  given high electrostatic repulsion from the layer containing Fe and S atoms along c-axis.<sup>2</sup> Although similar pathway-energy profile is observed for experimental structural model, it corresponds to a 1D pathway which may be an artefact from BVSE calculation. Structural illustration performed using VESTA® software.

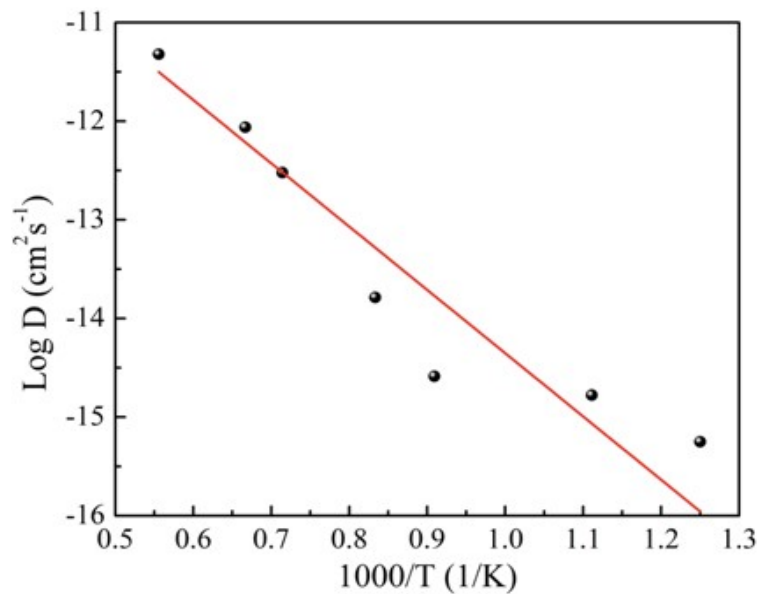


**Fig. S5.** Arrhenius plot for  $\text{LiNaV}(\text{SO}_4)_2$ . The Arrhenius plot for diffusion coefficients at temperatures of 800, 900, 1100, 1200, 1400, 1500 and 1800 K for  $\text{Li}^+$  diffusion. From Arrhenius plot, the value of activation energy  $E_a$  is 0.55 eV, which is needed for  $\text{Li}^+$  mobility in this material.

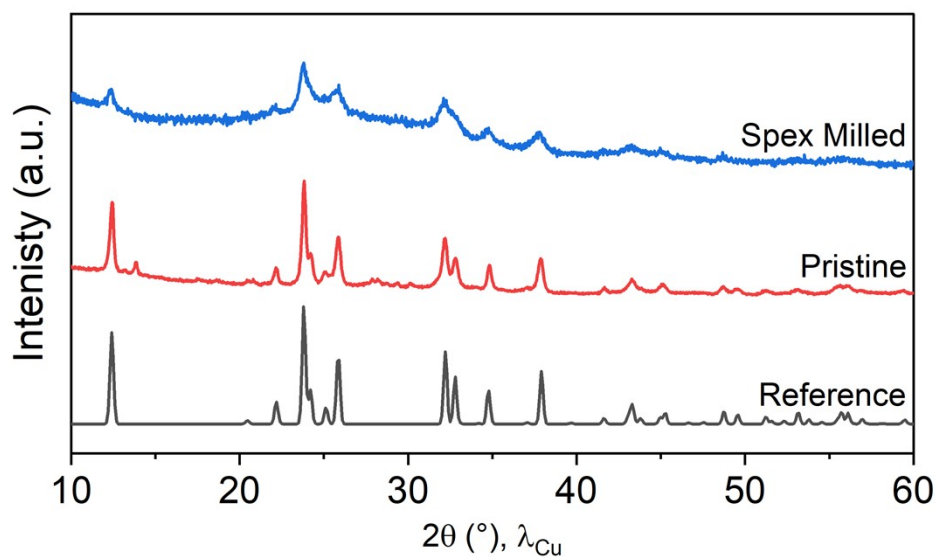


**Fig. S6.** Comparative powder diffractogram of reference (black), pristine (red) and milled mixture of  $\text{NaV}(\text{SO}_4)_2$  (blue) showcasing that the crystallinity of the material is intact after milling.

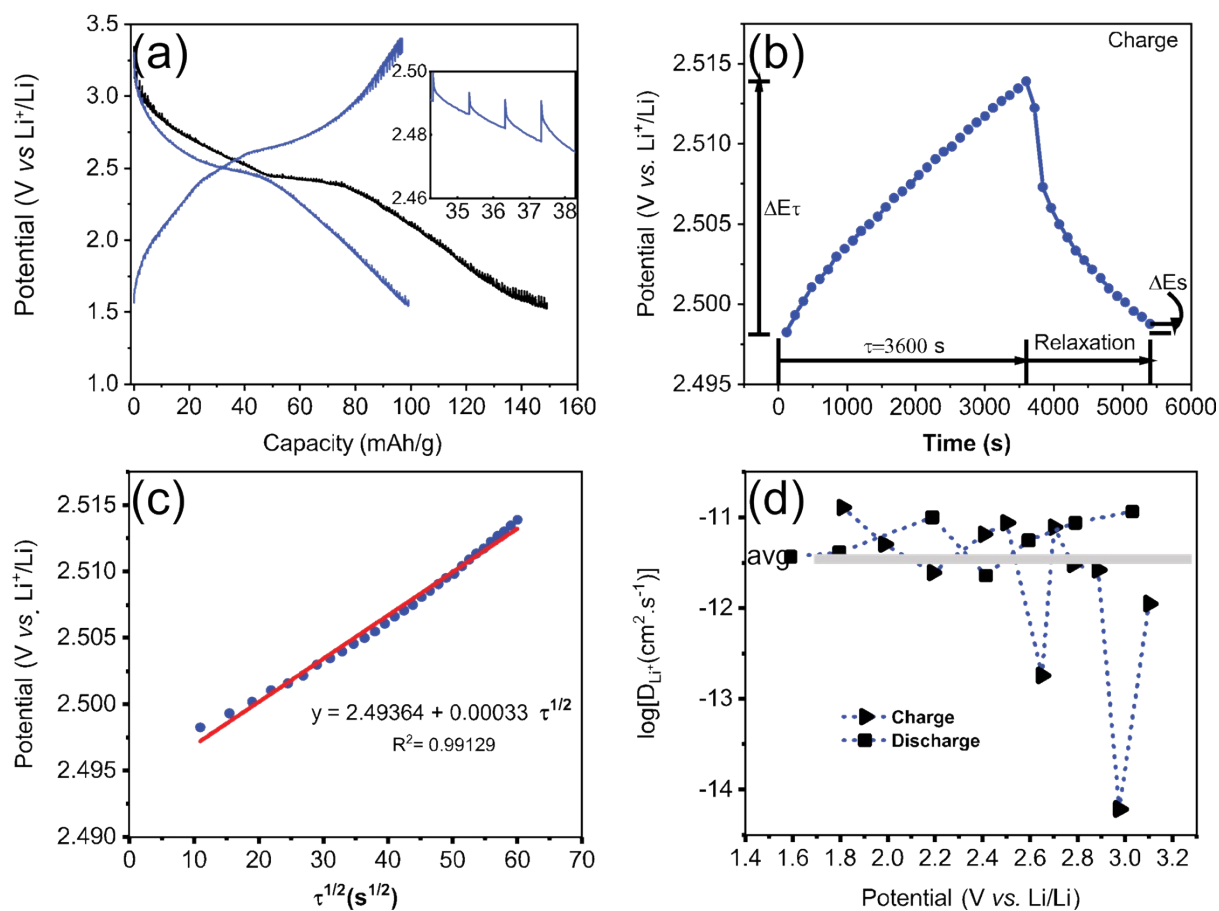


**Fig. S7.** For the half cell:  $\text{NaV}(\text{SO}_4)_2 | 1\text{M LiClO}_4 \text{ in PC} | \text{Li}$ . (a) Galvanostatic intermittent titration performed at a current rate of  $C/100$  with intermittent (dis)charging step of 1 h between 1.5-3.4 V (b) a representative potential vs. time profile during charging process depicting  $\Delta E\tau$ ,  $\tau$ , relaxation time and  $\Delta E_s$  parameters (c) Linear behavior of Potential vs.  $\tau^{1/2}$  (d)  $\text{Li}^+$  diffusion coefficient calculated using simplified application of Fick's second law. The grey strip is guide for the eye at  $\text{Li}^+$  diffusion  $\tau$  coefficient of the order of  $10^{-11.5} \text{ cm}^2/\text{s}$ .

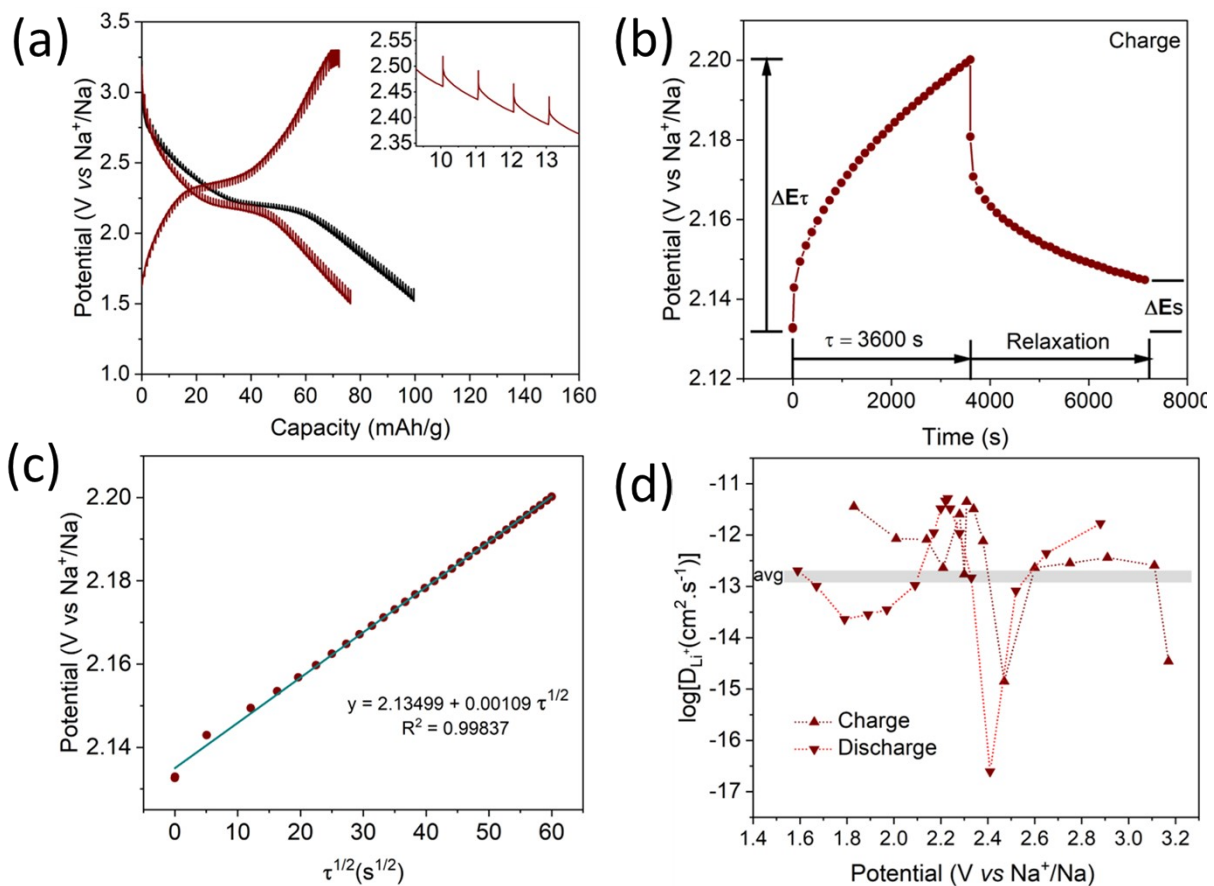


**Fig. S8.** For the half cell:  $\text{NaV}(\text{SO}_4)_2 | 1\text{M NaClO}_4$  in  $\text{EC/PC/DMC} | \text{Na}$ . (a) Galvanostatic intermittent titration performed at a current rate of  $C/100$  with intermittent (dis)charging step of 1 h between 1.5-3.4 V (b) a representative potential vs. time profile during charging process depicting  $\Delta E\tau$ ,  $\tau$ , relaxation time and  $\Delta E_s$  parameters (c) Linear behavior of Potential vs.  $\tau^{1/2}$  (d)  $\text{Na}^+$  diffusion coefficient calculated using simplified application of Fick's second law. The grey strip is guide for the eye at  $\text{Na}^+$  diffusion coefficient of the order of  $10^{-13} \text{ cm}^2/\text{s}$ .

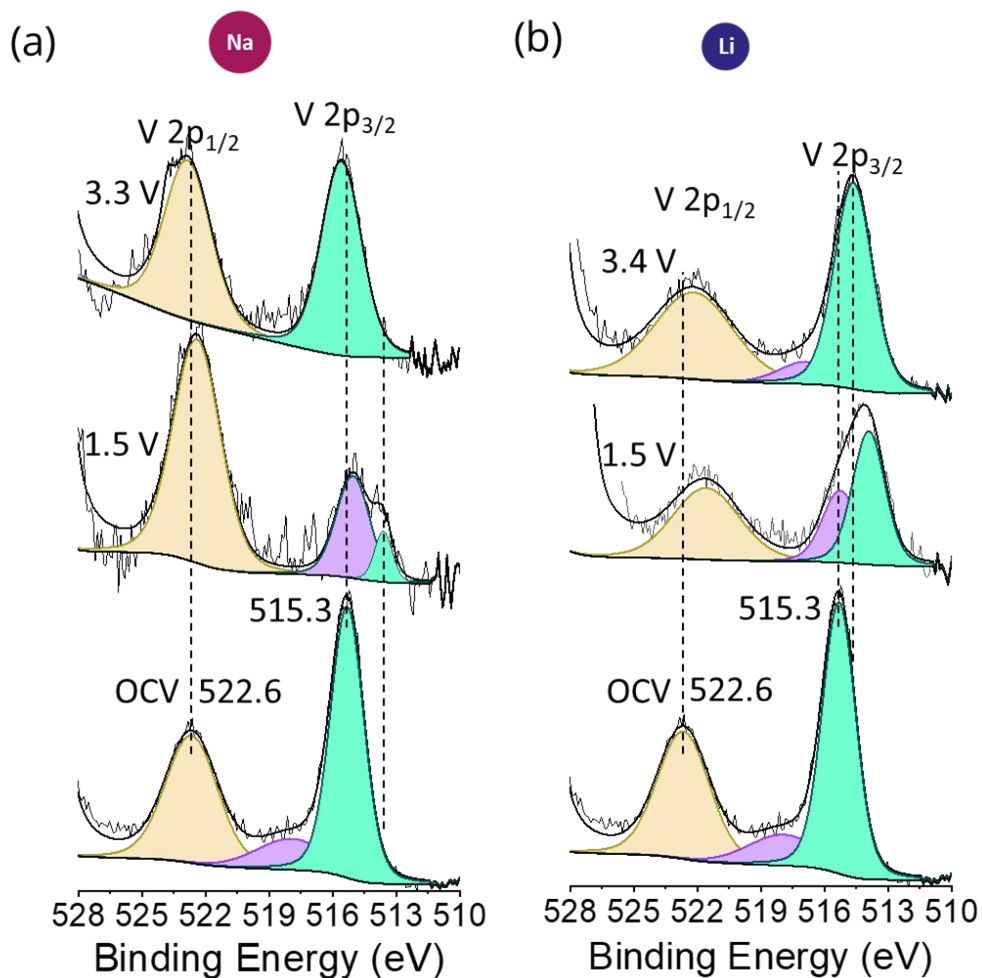


**Fig. S9.** Postmortem analyses. *Ex situ* XPS V(2p) spectra for (a) Na, and (b) Li half cells fitted in conjunction with O(1s) spectra (not shown) for improved overall fitting.<sup>3</sup> Cells were disconnected at three potentials (1.5 V, 2.4 V and 3.4/3.3 V) in the voltage range 1.5-3.4 V.

#### References:

1. K. Momma and F. Izumi, *J. Appl. Crystallogr.*, 2011, **44**, 1272.
2. A. Banerjee, R. B. Araujo and R. Ahuja, *J. Mater. Chem. A*, 2016, **4**, 17960.
3. G. Silversmit, D. Depla, H. Poelman, G. B. Marin and R. De Gryse, *J. Electron. Spectrosc. Relat. Phenom.*, 2004, **135**, 167.